JOURNAL OF VIROLOGY, Jan. 2005, p. 106–115 Vol. 79, No. 1
0022-538X/05/$08.00+0 doi:10.1128/JVI.79.1.106–115.2005

The Cytoplasmic Tail Slows the Folding of Human Immunodeficiency Virus Type 1 Env from a Late Prebundle Configuration into the Six-Helix Bundle

Levon G. Abrahamyan,[1] Samvel R. Mkrtchyan,[1] James Binley,[2] Min Lu,[3] Grigory B. Melikyan,[1] and Fredric S. Cohen[1]*

Department of Molecular Biophysics and Physiology, Rush University Medical Center, Chicago, Illinois[1]; Torrey Pines Institute for Molecular Studies, San Diego, California[2]; and Department of Biochemistry, Weill Medical College of Cornell University, New York, New York[3]

Received 17 May 2004/Accepted 18 August 2004

Effects of the cytoplasmic tail (CT) of human immunodeficiency virus type 1 Env on the process of membrane fusion were investigated. Full-length Env (wild type [WT]) and Env with its CT truncated (ΔCT) were expressed on cell surfaces, these cells were fused to target cells, and the inhibition of fusion by peptides that prevent Env from folding into a six-helix bundle conformation was measured. For both X4-tropic and R5-tropic Env proteins, ΔCT induced faster fusion kinetics than did the WT, and peptides were less effective at inhibiting ΔCT-induced fusion. We tested the hypothesis that the inhibitory peptides were less effective at inhibiting ΔCT-induced fusion because ΔCT folds more quickly into a six-helix bundle. Early and late intermediates of WT- and ΔCT-induced fusion were captured, and the ability of peptides to block fusion when added at the intermediate stages was quantified. When added at the early intermediate, the peptides were still less effective at inhibiting ΔCT-induced fusion but they were equally effective at preventing WT- and ΔCT-induced fusion when added at the late intermediate. We conclude that for both X4-tropic and R5-tropic Env proteins, the CT facilitates conformational changes that allow the trimeric coiled coil of prebundles to become optimally exposed. But once Env does favorably expose its coiled coil to inhibitory peptides, the CT hinders subsequent folding into a six-helix bundle. Because of this facilitation of maximal exposure and hindrance of bundle formation, the coiled coil is optimally exposed for a longer time for WT than for ΔCT. This accounts for the greater peptide inhibition of WT-induced fusion.

The envelope protein (Env) of human immunodeficiency virus (HIV) is a potential target for vaccines and drug therapies. Blocking formation of the six-helix bundle (6HB) structure of Env has been shown to be an effective means of preventing HIV infection (for a review, see reference 16). As has been observed from Env's postfusion structure, its 6HB is formed from three C-terminal and three N-terminal heptad repeat regions of the trimeric transmembrane subunit gp41 (9, 55, 56). The N-terminal segments form a central triple-stranded coiled coil, and at a late stage of fusion (42), the C-terminal segments pack, antiparallel to the N segments, into the hydrophobic grooves on the surface of the coiled coil, completing the 6HB. T20, a synthetic 36-residue peptide that is derived from the C-terminal heptad region, binds to the grooves of the coiled coil and prevents infection by blocking formation of the 6HB (see, for example, references 5, 10, and 15). The T20 peptide (32) has recently been approved by the Food and Drug Administration and is prescribed under the brand names Fuzeon and Enfuvirtide. Other synthetic peptides that duplicate the C-terminal heptad repeat regions (e.g., C34) act in a similar manner. In the native structure of Env, the grooves are not exposed (in fact, the coiled coil may not have yet been formed) but become transiently exposed during the fusion process; inhibitory peptides can therefore block infection only if they fill the grooves during this window of exposure.

HIV isolates exhibit considerable variability in their sensitivity to T20 and other 6HB inhibitory peptides (2, 12, 13, 36). As a rule, isolates that use the chemokine receptor CCR5 as a coreceptor are more resistant to inhibitory peptides than are laboratory-adapted strains that use CXCR4 (12, 13). Understanding the molecular basis for differences in inhibitory peptide sensitivity could therefore be important in ensuring effective antiviral therapy. The association between tropism and inhibitory peptide sensitivity may be related to a much higher binding affinity of R5-tropic Env to CCR5 than of X4-tropic Env to CXCR4 (see reference 14 and references therein). Tropism is primarily determined by the amino acid sequence of the V3 loop (see, for example, reference 53). Studies have shown that replacing the V3 loop of a laboratory-adapted X4-tropic HIV type 1 (HIV-1) Env protein with that of an R5-tropic primary isolate yields a chimeric construct that is R5 tropic (12, 13, 26, 27, 29). This chimeric Env protein bound CCR5 with high affinity and exhibited resistance to T20, characteristic of the R5-tropic Env protein from which the V3 loop was derived (12, 13, 48). In general, as the affinity between such chimeric Env constructs and chemokine receptors increases, fusion kinetics also increase and the efficacy of T20 decreases (48). It has been proposed that higher affinity between Env and chemokine receptors causes quicker folding of Env and therefore faster fusion kinetics and that quicker folding of Env from prebundle configurations into a 6HB shortens the time of ex-

* Corresponding author. Mailing address: Department of Molecular Biophysics and Physiology, Rush University Medical Center, 1653 W. Congress Pkwy., Chicago, IL 60612. Phone: (312) 942-6753. Fax: (312) 942-8711. E-mail: fcohen@rush.edu.

posure of binding sites, accounting for the greater resistance to T20 (20, 48).

Among enveloped viruses, HIV Env has an unusually long cytoplasmic tail (CT), ~150 residues. The CT is thought to modulate several of the steps in viral entry. When HIV-2 or simian immunodeficiency virus (SIV) is grown in tissue culture, a spontaneous truncation of the CT occurs that markedly improves the virus's ability to grow (8, 25). In addition, the presence of the CT appears to affect the receptor requirement: HIV-1 or HIV-2 grown in cell lines devoid of Env's receptor (CD4), but expressing the appropriate chemokine receptors, tends to naturally develop Env proteins with truncated CTs, as the virus reverts to CD4-independent fusion (17, 35, 37, 49). In fact, a shortened CT is a common—although far from universal—feature of CD4-independent Env (18).

In the present study, we investigated fusion activities caused by wild-type (WT) HIV-1 Env and an Env protein in which the CT was deleted (ΔCT). We expressed the R5-tropic and X4-tropic WT and ΔCT of HIV-1 in effector cells and fused them to target cells that express CD4 and appropriate chemokine receptors. By arresting fusion at intermediate stages, we tested whether differences in sensitivity to inhibitory peptides between WT- and ΔCT-induced fusions are controlled by folding kinetics; we identified the transitions between intermediate states that were strongly affected by the CT. We found that deleting the CT had two major effects: it increased the rate of fusion, and it rendered Env more resistant to peptides that block 6HB formation. For both WT and ΔCT, we created fusion intermediates to stably expose the inhibitory peptide binding sites, thereby eliminating the window of time for binding as a factor in the inhibition of fusion. We found that the peptides were equally effective at preventing WT-induced fusion and ΔCT-induced fusion when added at an advanced stage. We define the transitory configurations of gp41 that maximally expose peptide binding sites as "late prebundle" conformations. We conclude that the time gp41 remains in these conformations is the major determinant for the differences in potency of inhibitory peptides to block WT- and ΔCT-induced fusions.

TABLE 1. WT and ΔCT expression in transfected cells

Env plasmid (amt, μg)[a]	IgG1b12 MAb		447-52D MAb		Fusion[c] (%)
	MFI[b]	Positive cells (%)	MFI	Positive cells (%)	
WT (10)	100 ± 12[d]	19.8 ± 2.7	100 ± 9	16.6 ± 1.6	18.5 ± 1.1
WT (4)	61 ± 6	11.8 ± 5.1	67 ± 4	8.2 ± 1.8	ND[e]
WT (2)	17 ± 3	4.7 ± 0.4	20 ± 2	4.0 ± 0.8	ND
ΔCT (10)	619 ± 22	49.7 ± 7.8	787 ± 13	46.5 ± 13.0	28.9 ± 2.2
ΔCT (4)	281 ± 10	24.1 ± 8.3	320 ± 6	19.8 ± 8.1	18.0 ± 2.6
ΔCT (2)	81 ± 6	19.9 ± 4.0	107 ± 1	15.1 ± 3.1	14.8 ± 0.8

[a] Amount of HXB2 Env-expressing plasmid used for transfection.
[b] MFI, mean fluorescence intensity normalized to that of 10 μg of the WT (after subtraction of the mean fluorescence intensity of mock-transfected cells).
[c] Fusion after correction for the background fusion observed for mock-transfected cells.
[d] The mean and standard error of the mean from at least three measurements are shown.
[e] ND, not determined.

MATERIALS AND METHODS

Cell lines and reagents. The 293T cell line was purchased from the American Type Culture Collection (Manassas, Va.). The TF228.1.16 cell line that stably expresses X4-tropic HIV-1 Env (31) was a generous gift from Z. Jonak (Glaxo SmithKline, Philadelphia, Pa.). HeLaT4$^+$ cells (40), provided by R. Axel, and 3T3.T4.CXCR4 and 3T3.T4.CCR5 cells, provided by D. Littman (11), were obtained through the AIDS Research and Reference Reagent Program, National Institute of Allergy and Infectious Diseases, National Institutes of Health. Cells were grown as described previously (42, 44).

Bovine serum albumin and poly-L-lysine were purchased from Sigma Chemical Co. (St. Louis, Mo.); lauroyl-lysophosphatidylcholine (LPC) was bought from Avanti Polar Lipids (Alabaster, Ala.). All fluorescent dyes—calcein AM, CMTMR {5 [and 6-]-(((4-chloromethyl)benzoyl)amino)-tetramethylrhodamine}, and CMAC (7-amino-4-chloromethylcoumarin)—were purchased from Molecular Probes (Eugene, Oreg.). The HIV gp120 monoclonal antibody (MAb) IgG1b12 (7) was provided by D. Burton and Carlos Barbas, and the 447-52D anti-V3 loop MAb (23) was provided by Susan Zolla-Pazner, both through the AIDS Research and Reference Reagent Program. The HIV gp41-derived inhibitory peptide C34 (sequence: WMEWDREINNYTSLIHSLIEESQN QQEKNEQELL) was synthesized by Macromolecular Resources (Fort Collins, Colo.). The untagged 5-helix peptide was constructed as previously described (44). It was expressed in *Escherichia coli* BL21(DE3)/pLysS with a modified pET3a vector (Novagen). The cells were harvested by centrifugation 4 h postinduction with 0.5 mM isopropyl-β-D-thiogalactopyranoside (IPTG), and the pellets were resuspended in 50 ml of buffer A (50 mM Tris [pH 8.0], 1 mM EDTA) plus 25% sucrose. The cells were lysed by sonication and centrifuged (35,000 × *g* for 30 min) to separate the soluble fraction from inclusion bodies. The inclusion bodies were subsequently washed extensively with buffer A plus 1% Triton X-100. The five-helix peptide was purified directly from the inclusion bodies resuspended in 8 M urea–buffer A. The debris was removed by a 1-h centrifugation at 4°C. The protein was then loaded onto a DEAE-Sepharose column (Amersham Pharmacia Biotech) equilibrated with buffer A plus 3 M urea and eluted with an NaCl gradient (0 to 500 mM) in buffer A plus 3 M urea. The five-helix peptide was refolded by step dialysis in buffer A with decreasing amounts of urea at 4°C. The refolded 5-helix peptide was applied to a MonoQ column (Amersham Pharmacia Biotech) equilibrated with buffer A. The protein was eluted from the MonoQ resin with an NaCl gradient in buffer A. The sample was concentrated by ultrafiltration to 5 mg/ml and stored at 4°C. The protein was >95% pure as judged by sodium dodecyl sulfate-polyacrylamide gel electrophoresis and is properly folded in terms of secondary structure and monomeric state (as judged by circular dichroism and sedimentation equilibrium experiments). Stock solutions of the inhibitory peptides were prepared in phosphate-buffered saline, aliquoted, and stored at −20°C.

Transient expression of HIV-1 Env. HIV-1 Env was expressed in 293T cells by calcium phosphate transfection. WT and ΔCT JRFL Env proteins were expressed with the pCAGGS plasmid (46). For the JRFL ΔCT construct, residues C terminal to V708 (by standard LAI numbering) were deleted, so that only three residues (NRV) of the CT remained. This construct has been described previously (4). The pSRHS vectors encoding the WT and ΔCT HXB2 Env proteins were obtained from E. Hunter (University of Alabama) (38). In HXB2 ΔCT, a 147-residue-long segment was deleted from the C terminus of gp41, leaving only four residues, NRVR, in the cytoplasmic segment. To match the expression densities of the WT and ΔCT proteins, the amount of ΔCT plasmid used for transfection was reduced severalfold with respect to that of the WT plasmid (which was usually added at 10 μg/6-cm-diameter dish). The amounts of plasmid used to match WT and ΔCT densities on the positive cells also led to the same percentages of cells expressing the WT and ΔCT proteins (Table 1). Adding less plasmid to lower the protein density on the surfaces of the transfected cells also reduced the percentage of cells expressing Env. Surface densities therefore could not be lowered too much without greatly increasing the percentage of nonexpressing cells. The Env surface expression levels were quantified essentially as described in reference 42, with 447-52D or IgG1b12 MAbs. The 447-52D antibody recognizes a short peptide at the apex of the V3 loop of gp120 (34, 54) and thus should bind equally well to WT and to conformationally altered ΔCT (18). Cells were analyzed in an ORTHO Cytoron Absolute flow cytometer (Ortho Diagnostic Systems, Raritan, N.J.).

Measurements of cell-cell fusion. Fusion was measured by two techniques: two-color fluorescence microscopy and flow cytometry. For fluorescence microscopy, as has been described in detail (42–44), effector cells expressing HIV-1 Env were loaded with calcein (green emission) and target cells expressing CD4 and coreceptor were loaded with CMAC (blue emission). Fusion events were scored as the appearance of cell pairs that were positive for both dyes, normalized by the total number of effector and target (E-T) cells in contact plus fused cells. The flow cytometry-based assay to measure cell-cell fusion induced by HIV-1 Env was

similar to assays described previously (28, 30, 57). Effector cells loaded with the green cytoplasmic dye calcein AM were laid on top of target cells loaded with the orange cytoplasmic dye CMTMR. The amounts of loaded calcein and CMTMR were adjusted so that excitation by the 488-nm laser of the flow cytometer yielded comparable emission signals from the two dyes. Cells were coincubated at 37°C, washed (to remove the unbound effector cells), and lifted off the dish by brief treatment with 0.5 mg of trypsin per ml and 0.5 mM EDTA in divalent-free phosphate-buffered saline (Gibco BRL). The last step stopped the fusion reaction and, most importantly, dispersed the unfused E-T cell pairs and aggregates that would otherwise produce a false double-positive cell population in flow cytometry. Bound but unfused E-T cells were, in practice, the primary cause of background signals. Trypsin cleavage was stopped by adding an excess of soybean trypsin inhibitor, and cell-cell fusion was quantified as the ratio of the double-positive cell population to the sum of the double-positive cells and the remaining target (orange) cells. By stopping the fusion reaction at different times and measuring the extents of fusion, we were able to determine the kinetics of fusion by flow cytometry which, to our knowledge, is a novel technique for measuring kinetics.

The percentage of fusion determined by flow cytometry was consistently lower than the percentage determined by fluorescence microscopy because of the method of calculation. In flow cytometry, the percentage is normalized by the total number of target cells, whereas in fluorescence microscopy, the percentage is normalized by the total number of bound target cells, which is always less than the total number of target cells. The efficacy of HIV fusion inhibitors under different sets of conditions was parameterized by determining 50% inhibitory concentrations (IC_{50}s) as described in reference 43. Briefly, dose-response data were fit with a Langmuir isotherm as follows: $F = F_0/(1 + C_i/IC_{50})$, where F_0 is the extent of fusion in the absence of an inhibitor (taken as 100%) and C_i is the inhibitor concentration. IC_{50} was chosen to minimize least-square deviation.

Fusion intermediates. Coincubating E-T cells for 2.5 h at 23°C, a temperature that does not permit fusion, kinetically advances the fusion process to a temperature-arrested stage (TAS) at which Env has undergone conformational changes that allow bundle-blocking peptides to bind gp41 (44). Adding 0.15 mg of LPC per ml after reaching the TAS, waiting 3 min at 23°C, warming the cells to 37°C for 15 min, lowering the temperature to 4°C, and then removing the LPC by washing the cells twice with medium containing bovine serum albumin yields a lipid-arrested stage (LAS) of fusion. When creating the LAS, fusion does not occur. To test the efficacy of C34 or the 5-helix peptide when added at the LAS, the peptides were added at 4°C, followed by a 30-min incubation at 23°C. Fusion did not occur during the incubation. The temperature was then raised to 37°C, and the extent of fusion was measured.

Immunoprecipitation of cell surface-expressed Env. The extent of proteolytic cleavage of gp160 into gp120/gp41 was assessed as described previously (1). Briefly, cell surface proteins were biotinylated and cells were lysed. The total amount of protein was determined (by a Bio-Rad protein assay kit), samples were adjusted to contain equal concentrations of protein, and Env was immunoprecipitated with HIV immune serum (from G. Spear, Rush University Medical Center). The immune complexes were separated by sodium dodecyl sulfate-polyacrylamide gel electrophoresis. The biotinylated Env was visualized by horseradish peroxidase-conjugated streptavidin (Pierce, Rockford, Ill.) with an ECL kit (Amersham-Pharmacia Biotech, Little Chalfont, Buckinghamshire, United Kingdom).

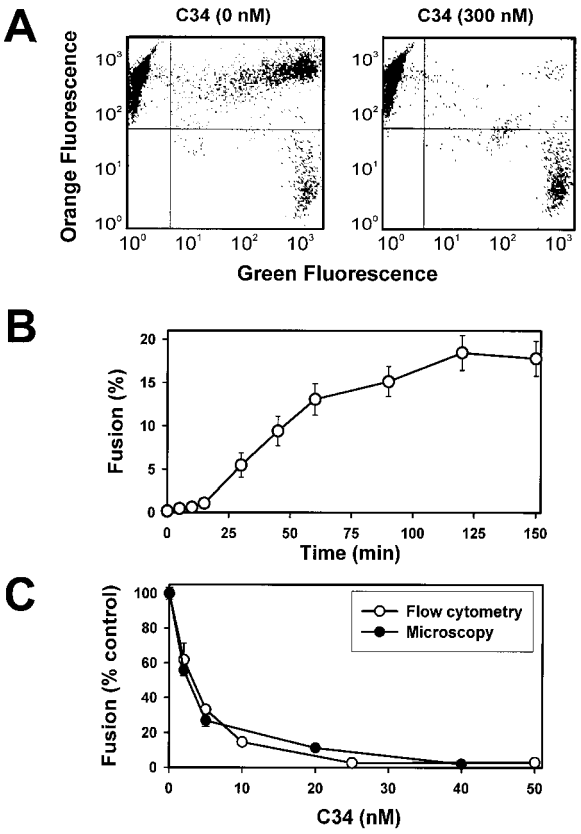

FIG. 1. Flow cytometry analysis of fusion between TF228.1.16 (effector) and HeLaT4$^+$ (target) cells. (A) Effector cells loaded with green cytoplasmic marker were coincubated with target cells loaded with orange marker for 2.5 h at 37°C either in the presence (right) or in the absence (left) of 300 nM C34 peptide. (B) Kinetics of cell-cell fusion were obtained by varying the time E-T cells were coincubated at 37°C, lowering the temperature to halt further fusion, and then lifting cells off the culture dishes with a trypsin-EDTA solution. (C) Dose-response curves for C34 inhibition measured by flow cytometry (open circles) and microscopy (filled circles) assays. A small background signal not related to fusion (about 1.5% of the total number of effector cells) was subtracted from the data in panels B and C. Unless stated otherwise, error bars represent standard errors of the mean for at least three independent duplicate measurements.

RESULTS

Flow cytometry reliably measures the extent and kinetics of cell-cell fusion. In this study, we quantified membrane fusion by flow cytometry and fluorescence microscopy. In initial experiments, we loaded effector TF228.1.16 cells (stably expressing HIV-1 Env) with a green dye (calcein) and fused them to target HeLaT4$^+$ cells (stably expressing CD4 and CXCR4) that were loaded with an orange dye (CMTMR). We chose these E-T cell pairs because we had already characterized their kinetics and fusion intermediates in considerable detail by fluorescence microscopy (42, 44). We could therefore compare fusion obtained by fluorescence microscopy and flow cytometry to ensure that results were independent of methodology. As determined by flow cytometry, incubating these E-T cells together at temperatures at or below 23°C did not yield fusion (e.g., see Fig. 3B); two distinct populations of cells, one green and one orange, were observed. In contrast, coincubating E-T cells at 37°C yielded a population of cells that were labeled by both dyes, denoting cell-cell fusion (Fig. 1A, left side). Typically, about 15% of the HelaT4 cells fused to TF228.1.16 cells (as determined by flow cytometry). As expected, a high concentration of the C34 peptide (added to E-T cells at the time of coincubation) completely eliminated double-labeled cells, showing that fusion was inhibited (Fig. 1A, right side). Also, effector cells cocultivated with CD4$^+$ target cells that express the noncognate CCR5 did not produce detectable fusion (data not shown). Flow cytometry has been used previously in similar manners to measure extents of fusion (28, 30, 38, 57).

We used the flow cytometry assay in a manner that allowed us to obtain the kinetics of cell-cell fusion (see Materials and Methods). We found that the kinetics were similar to the kinetics we previously obtained for the same cell pairs by using

fluorescence microscopy as the assay (44): a 20-min lag time and ~2 h to reach a maximal extent of fusion (Fig. 1B). To further validate the quantitative reliability of the flow cytometry assay, we compared its determination of the dose dependence of inhibition of fusion by C34 peptide against that determined by the fluorescence microscopy assay (43). The two assays were in good quantitative agreement (Fig. 1C). We used both assays to compare fusions induced by the WT and ΔCT proteins.

Fusion kinetics of HIV Env is augmented by deletion of its CT. A flow cytometric analysis showed that for the same concentration of plasmid in transfection, the ΔCT protein was expressed on the surfaces of cells at significantly higher densities than was the WT protein. This was observed for both X4-tropic HXB2 Env (Table 1) and R5-tropic JRFL Env (data not shown). A higher density is expected because deletion of the tail eliminates an internalization signal (YXXL) (6).

The extent of fusion induced by the ΔCT protein was greater than that induced by the WT protein; this would be expected because of the higher expression levels of the ΔCT protein (Table 1 and reference 39). In order to meaningfully compare fusions induced by the WT and ΔCT proteins, we reduced the amount of ΔCT-bearing plasmid used for transfection (see Materials and Methods) until the densities of the WT and ΔCT plasmids were matched. For HXB2 Env, reducing the concentration of the ΔCT plasmid fivefold with respect to that of the WT plasmid (2 μg of ΔCT plasmid versus 10 μg of WT plasmid) yielded comparable surface densities and similar extents of cell-cell fusion after a 2-h coincubation at 37°C (Table 1). However, the ΔCT plasmid induced faster fusion kinetics than did the WT plasmid (Fig. 2). This was the case for both R5-tropic Env (JRFL, Fig. 2A) as determined by fluorescence-activated cell sorter analysis and X4-tropic Env (HXB2, Fig. 2B) as determined by microscopy. In separate experiments, we found that the temperature thresholds were comparable for ΔCT-induced and WT-induced fusions for both JRFL (Fig. 3A) and HXB2 (Fig. 3B). The lowest temperature necessary for fusion was less for JRFL than for HXB2 (Fig. 3).

Since it was possible that the faster kinetics of ΔCT-induced fusion were due to more-efficient cleavage into gp120 and gp41 subunits (which would increase the density of Env capable of inducing fusion), we biotinylated surface-expressed Env, immunoprecipitated it with pooled human HIV-containing sera, and analyzed the immune complexes by Western blotting. We found that both the WT and ΔCT gp160 precursors were properly and almost completely cleaved into two subunits, judging from the relative intensities of gp160 and gp120 bands (Fig. 4). The extent of cleavage of gp160 was, however, somewhat greater for ΔCT. This indicates that either the cleavage site within the ectodomain was more exposed or the time for cleavage during intracellular trafficking was greater for ΔCT. It had been previously found that MAbs directed against gp120 epitopes normally exposed by CD4 recognize ΔCT much better than the WT when CD4 is not present (18). Therefore, the CT appears to modulate the structure of the ectodomain of Env.

Although we found comparable expression levels by flow cytometry, the apparent levels of ΔCT expression revealed by immunoprecipitation (followed by Western blotting) were significantly lower than those of the WT. If the ΔCT expression densities were lower than those of the WT, this would further emphasize that the CT of Env slows fusion. Factors other than surface density and proteolytic processing of Env appear to render ΔCT more fusogenic. In short, the absence of the CT speeds the kinetics of fusion and does so without appreciably altering the efficiency of proteolytic processing.

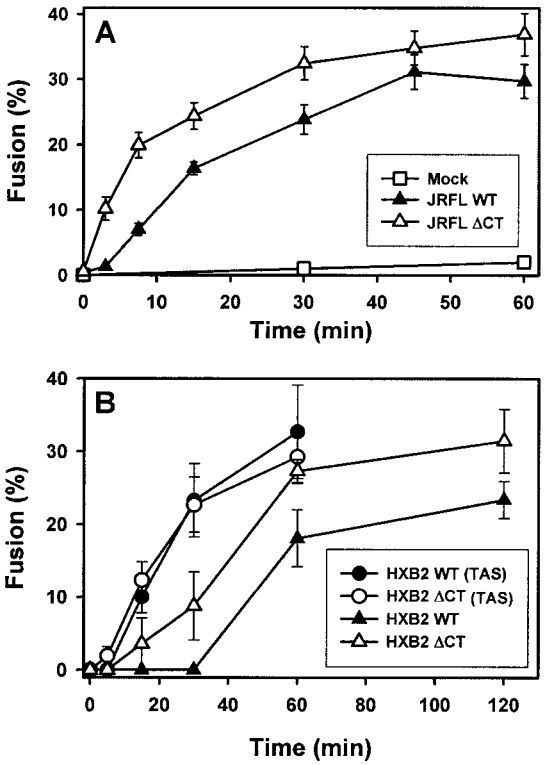

FIG. 2. Kinetics of cell-cell fusion induced by the WT and ΔCT. (A) Fusion between 293T cells transiently expressing JRFL WT (filled triangles) or ΔCT (open triangles) and target 3T3.CD4.CCR5 cells was monitored by the flow cytometry assay as described in the legend to Fig. 1. Open squares are the background signal, as observed with mock-transfected 293T cells. (B) The kinetics of fusion induced by HXB2 WT (filled symbols) or ΔCT (open symbols) transiently expressed in 293T and HeLaT4$^+$ cells were measured by fluorescence microscopy. Fusion was induced by coculturing the cells either directly at 37°C (triangles) or after preincubation at 23°C for 2.5 h (circles).

Deletion of the Env CT reduces the effectiveness of fusion inhibitory peptides. It has been found that an increased rate of HIV Env-induced fusion tends to correlate with reduced potency of peptides that inhibit fusion by preventing 6HB formation (48). We therefore determined the relative abilities of the C34 and 5-helix peptides to suppress cell-cell fusion induced by the WT and ΔCT proteins. C34 inhibits bundle formation by binding to the N-terminal heptad repeat region (i.e., the coiled coil) of gp41 (16); the recombinant 5-helix peptide has a triple-stranded coiled coil with only one vacant groove, and it inhibits bundle formation by binding to the C-terminal heptad repeats of Env (50, 51). By measuring the dose dependence of inhibition of fusion, we found that the ΔCT protein (Fig. 5, closed symbols) was substantially more resistant to both the C34 (Fig. 5A) and 5-helix (Fig. 5B) peptides than was the WT (open symbols). Such was the case for both the X4-tropic HXB2 (triangles) and R5-tropic JRFL (circles) Env proteins. For example, for HXB2, the IC_{50} was approximately fivefold higher

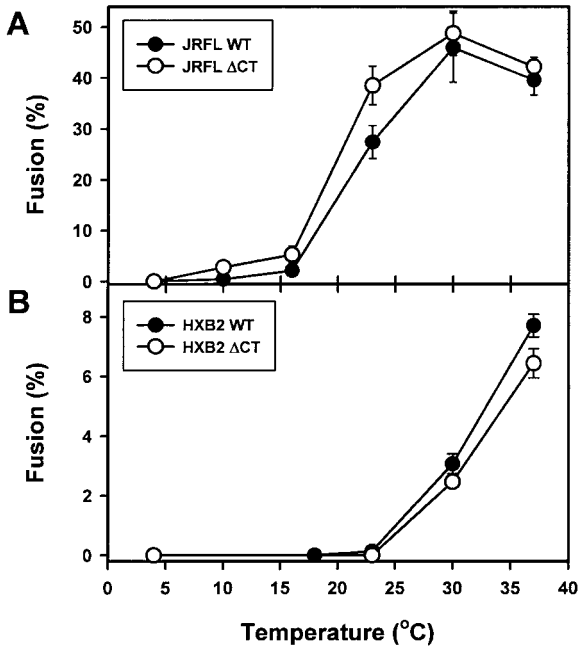

FIG. 3. Temperature dependence of fusion promoted by the WT (filled symbols) and ΔCT (open symbols) from the JRFL (A) and HXB2 (B) strains. Cells were coincubated for 2.5 (HXB2) or 2 (JRFL) h at the indicated temperature and then analyzed by flow cytometry. The extent of fusion induced by JRFL Env at 37°C was determined after a 1 h of incubation to reduce the formation of large syncytia. The background signal (<2% of the effector cells after a 37°C incubation) was subtracted from the plotted data. The apparent reduced fusion of JRFL Env at 37°C was caused by leakage of calcein from the effector cells and by syncytium formation, as verified by fluorescence microscopy (data not shown).

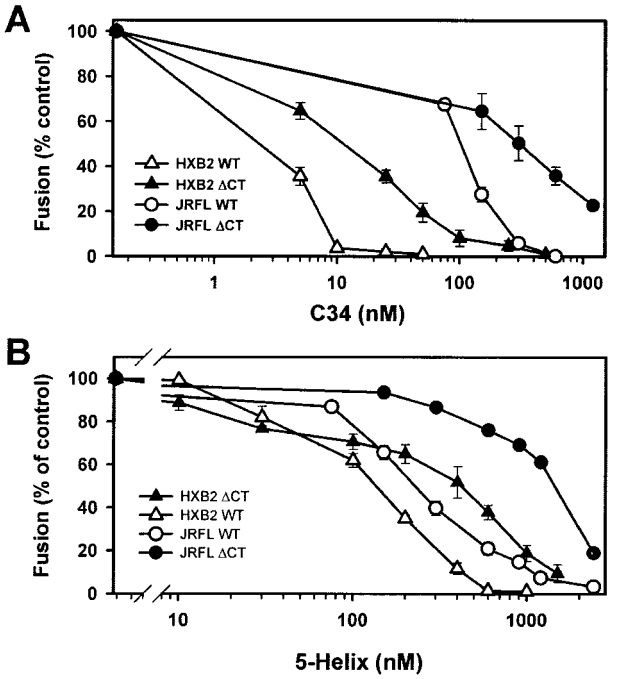

FIG. 5. Inhibition of HIV Env-induced cell-cell fusion by the C34 (A) and 5-helix (B) peptides. 293T cells expressing JRFL (circles) or HXB2 (triangles) were coincubated with appropriate target cells in the presence of varied concentrations of HIV fusion inhibitors for 1 or 2.5 h, respectively. WT-induced fusion (open symbols) was more sensitive to inhibitors than was fusion induced by ΔCT (filled symbols). Fusion was quantified by flow cytometry.

for C34 (Fig. 5A and 6A) and approximately threefold higher for the 5-helix peptide for ΔCT-induced fusion (Fig. 5B and 7A). Much higher concentrations of the C34 and 5-helix peptides were required to inhibit JRFL-induced than HXB2-induced fusion (Fig. 5). The fusion kinetics were faster for JRFL than for HXB2 (Fig. 2). Our results are in accord with a previous demonstration that, compared to the WT, an Env protein with a shortened CT (referred to as "8X" [17, 35]) exhibits faster cell-cell fusion and a reduced ability of T20 to inhibit fusion (20).

The efficacy with which C34 inhibited fusion decreased when the expression level of Env was increased. For HXB2, doubling the amount of plasmid used for transfection raised the IC_{50} of C34 for ΔCT-induced fusion from 12 to 26 nM (Table 2). For JRFL, tripling the amount of plasmid increased the IC_{50} of C34 against ΔCT-induced fusion from ~300 to ~730 nM (Table 2). The finding that more C34 is required to inhibit fusion as the density of Env increases was expected: IC_{50} is the concentration of peptide that blocks 50% of the fusion events, not the concentration that prevents 50% of the copies of Env from folding into a 6HB. Because higher expression levels should yield more potential fusion sites between cell pairs, a higher peptide concentration should be needed to block fusion. In summary, we have found a correlation between resistance against inhibitory peptides and fusion kinetics, as previously reported by others (20, 48), as well as a correlation between peptide inhibition and density of Env. For the remainder of this study, we primarily used HXB2 Env because we had previously characterized intermediate stages of its fusion in some detail (42, 44).

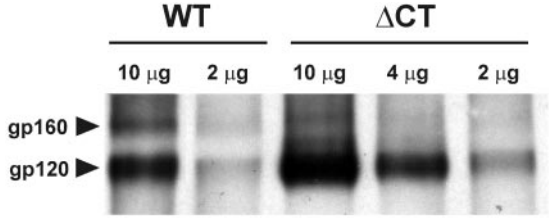

FIG. 4. Efficiency of proteolytic cleavage of cell surface-expressed HXB2 WT and ΔCT. The amounts of WT- and ΔCT-bearing plasmids used to transfect a 6-cm-diameter dish of 239T cells are indicated above the lanes. For details, see Materials and Methods.

The resistance of ΔCT and WT proteins to inhibitory peptides is the same at the LAS. We arrested fusion at intermediate stages so that the binding sites for the C34 and 5-helix peptides on gp41 were exposed. We reasoned that if inhibitory peptides were less effective at blocking ΔCT-induced fusion because ΔCT more rapidly folded into a 6HB, addition of the C34 and 5-helix peptides after creating the intermediates should inhibit fusion of the WT and ΔCT proteins to the same extent. We verified by fluorescence microscopy that the process of fusion between 293T cells transiently expressing HXB2 Env and HeLaT4$^+$ cells was kinetically advanced at the TAS

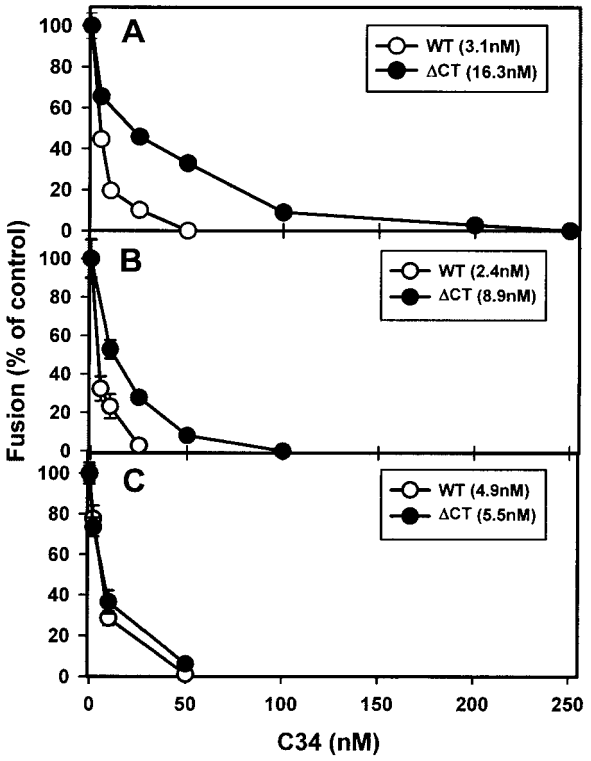

FIG. 6. Efficacy of C34 peptide at sequential intermediate stages of fusion induced by HXB2 WT (open circles) and ΔCT (filled circles). Varied concentrations of C34 were added either at the beginning of E-T cell coincubation (A), at the TAS (B), or at the LAS (C). Fusion was then triggered by incubating the cells at 37°C for 2.5 h (A) or for 1 h (B and C). The IC_{50}s obtained by curve fitting (see Materials and Methods) are given in parentheses in the insets. Fusion was quantified by fluorescence microscopy.

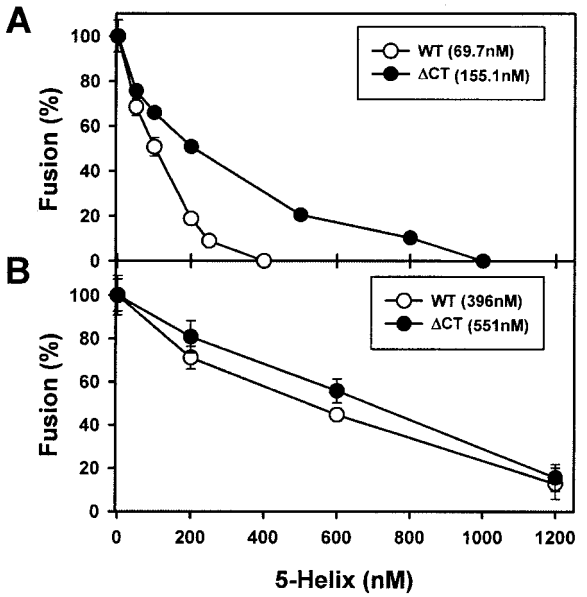

FIG. 7. Relative potency of the 5-helix peptide added at the beginning of E-T cell coincubation (A) or at the LAS (B). The IC_{50}s for the HXB2 WT (open circles) and ΔCT (filled circles) are given in parentheses. Details are given in the legend to Fig. 6.

(created by preincubation at 23°C for 2.5 h) by showing that a subsequent exposure to 37°C promoted faster fusion than that which occurred in control experiments in which the preincubation was omitted (Fig. 2B). Without prior cell coincubation, the kinetics of fusion was appreciably faster for the ΔCT protein than for the WT protein (Fig. 2B). C34 blocked WT-induced fusion more effectively than it blocked ΔCT-induced fusion (Fig. 6A). Thus, results obtained by fluorescence microscopy were in accord with the relative potencies of peptides determined by flow cytometry (Fig. 5). After creation of the TAS, the fusion rates were virtually identical for the WT and ΔCT proteins (Fig. 2B, open and closed circles) but C34 was still more effective at blocking WT fusion (Fig. 6B). C34 added at the TAS was not appreciably more effective at blocking WT-induced fusion (Fig. 6B) than when it was added at the start of coincubation (Fig. 6A), but ΔCT-induced fusion was more effectively inhibited by C34 added at the TAS than when it was added at the initiation of coincubation. (We refer to experiments in which E-T cells are continuously coincubated at 37°C as the control.) Thus, eliminating the time of binding for C34 as a factor did not alter the inhibition of fusion for the WT, but it increased the inhibition for ΔCT. In other words, the data indicate that when cells are coincubated immediately at 37°C, the WT exists in prebundle configurations long enough for effective binding of C34. But for ΔCT, grooves are more briefly exposed, for a time too short for C34 to bind maximally. It has been shown that fusion is inhibited after T20 is added and unbound peptide is then removed at the TAS (44). The finding that C34 was still not as effective at inhibiting ΔCT-induced fusion as at inhibiting WT-induced fusion (Fig. 6B) suggests that the grooves of the coiled coil of ΔCT were not maximally exposed at the TAS and that the prebundle configuration of ΔCT protein at the TAS folded into a 6HB more quickly than that of the WT protein.

The LAS intermediate is a more advanced intermediate than the TAS intermediate (44) (in fact, in this study the LAS intermediate was generated from the TAS intermediate [see Materials and Methods]). We created the LAS intermediate in order to test the relative sensitivities of WT- and ΔCT-induced fusions to the inhibitory peptides at a stage later than the TAS. If 6HBs do not form prior to pore formation (42, 44; see reference 22 for a counterview), a more advanced intermediate could increase the likelihood that peptide binding sites on the

TABLE 2. Susceptibility of fusion to C34 peptide depends on Env expression density in control experiments but not from the LAS

Env plasmid (amt, μg)[a]	IC_{50}, nM (control)[b]	IC_{50}, nM (from LAS)
JRFL WT (6)	46.9	ND[c]
JRFL ΔCT (2)	306.1	ND
JRFL ΔCT (6)	727.0	ND
HXB2 WT (10)	1.9	6.0
HXB2 ΔCT (2)	11.6	5.5
HXB2 ΔCT (4)	25.6	5.4

[a] Amount of Env-expressing plasmid used for transfection of 293T cells.
[b] C34 was added either at the beginning of coincubation of E-T cells (control) or after creation of the LAS. The extent of fusion was determined by flow cytometry as described in Materials and Methods.
[c] ND, not determined.

gp41prebundle become fully exposed. After creating the LAS intermediate, incubating cells at 37°C led to fusion. However, this extent was less than that which occurs by continuously coincubating E-T cells at 37°C and was somewhat less for the ΔCT protein than for the WT protein: compared to the fusion of control experiments, only ~70% of WT-expressing cells and ~50% of ΔCT-expressing cells fused from the state of the LAS, as determined by fluorescence microscopy. Adding C34 (Fig. 6C) at the LAS inhibited fusion in a dose-dependent manner when the temperature was raised to 37°C. At the LAS, C34 (Fig. 6C) was virtually as effective for WT-induced fusion as for ΔCT-induced fusion.

We tested whether the ability of C34 to equally inhibit WT- and ΔCT-induced fusions at the LAS is independent of Env density. C34 added after creation of the LAS inhibited fusion (induced by raising the temperature to 37°C) to the same extent for high and low expression levels of ΔCT; these IC_{50}s were comparable to that measured for the WT (Table 2). This indicates that ΔCT did not more readily inactivate than the WT during the experimental manipulations used to achieve LAS: greater inactivation could have caused ΔCT to produce a smaller number of fusion-competent sites than did the WT. This in turn could have increased the susceptibility of ΔCT-induced fusion to peptides to the point that peptide inhibition became comparable for ΔCT and the WT at the LAS. The equal efficacies of inhibitory peptides for ΔCT- and WT-induced fusions at the LAS, independent of density, are what one would expect if the time of exposure of binding sites determined the relative susceptibilities of WT- and ΔCT-induced fusions to inhibitor peptides. We are thus led to the key conclusion that the potency of inhibition of fusion by C34 is inherently the same for the WT and ΔCT; the difference between the two is caused by faster folding of ΔCT into 6HBs, limiting the time during which C34 can bind to the grooves of the coiled coil.

The potency of inhibition of WT-induced fusion by C34 was not affected by creation of the TAS or LAS, but C34 inhibited ΔCT-induced fusion more effectively at the LAS than at the TAS. This indicates that the grooves of the coiled coil of ΔCT were more exposed at the LAS than at the TAS. Creating the LAS also rendered the 5-helix peptide (Fig. 7B) almost equally effective at inhibiting WT- and ΔCT-induced fusions. But in contrast to C34, the IC_{50} for inhibition by the 5-helix peptide was significantly higher at the LAS (Fig. 7B) than at initial coincubation (Fig. 7A) for both the WT and ΔCT. We infer that the grooves created by N-terminal segments continue to be accessible (and quite possibly become more accessible), but the C-terminal segments become less accessible as fusion advances toward membrane merger. A similar phenomenon has been observed for the fusion protein of paramyxovirus SV5 (52).

DISCUSSION

Intermediates and peptide inhibitors provide a method for comparing the rate of folding of the WT and mutant Env proteins into a 6HB. Fusion induced by the WT exhibits slower kinetics and greater susceptibility to inhibition by C34 and the 5-helix peptide than that induced by ΔCT. If the slower fusion kinetics were predominantly due to the WT more slowly reconfiguring from a prebundle to a bundle, a more potent inhibition of fusion by peptide would be expected (48). But differences in fusion kinetics can have many different causes, and currently it is not possible to isolate each of these causes or to determine their relative importance, if any, to the fusion process. So the finding that ΔCT exhibits faster kinetics of fusion than the WT does not necessarily account for the reduced sensitivity of ΔCT to inhibitors of 6HB formation. Our strategy of creating stable intermediates and testing the potency of peptides against bundle formation at these stages allows one to bypass these kinetic uncertainties and to clearly determine the relative exposure of grooves at progressive stages of fusion. This methodology should also prove useful in future studies of the mechanism of inhibition of fusion by other reagents.

Greater resistance to peptide inhibitors is due to faster folding of ΔCT than the WT into 6HBs at a late stage of fusion. We found that when inhibitory peptides were added at the TAS and then maintained, they were more effective at blocking WT- than ΔCT-induced fusion, even though the kinetics of fusion from the TAS were the same for the WT and ΔCT. The IC_{50} of C34 for inhibition of WT-induced fusion was relatively independent of whether it was added at the beginning of cell coincubation, at the TAS, or at the LAS (Fig. 6). This indicates that the kinetics of refolding of the WT were sufficiently slow, or binding sites were sufficiently exposed, that C34 could bind according to its intrinsic affinity. Maintenance of inhibition also contradicts the claim that C34 loses potency at advanced fusion intermediates and that 6HBs form prior to membrane merger (22). Quantitative retention of fusion inhibition by C34 at the LAS is in accord with our prior conclusion that copies of Env that participate in fusion do not fold into bundles before membrane merger (44) and that bundle formation is not complete until after pore formation (42).

The advanced intermediate of the LAS had to be achieved in order for the inhibitory peptides to equally inhibit WT- and ΔCT-induced fusions. For ΔCT, the IC_{50} progressively decreased as C34 was added at the initial E-T cell coincubation at 37°C, at the TAS, and at the LAS. This suggests that binding of C34 to the grooves of the central coiled coil of ΔCT is restricted until the LAS is reached and that when fusion is allowed to proceed continuously rather than arrested at the LAS, the time of maximal groove exposure is limited. Taken together, the data indicate that ΔCT (Fig. 8, bottom panels) optimally exposes the grooves of its coiled coil later than does the WT (upper panels), but ΔCT more quickly folds into a 6HB from this point. As a result, the grooves are optimally exposed to C34 for longer times for the WT (upper panels). Thus, our data provide strong support for the hypothesis that faster folding of ΔCT, compared to that of the WT, from a late prebundle configuration into a 6HB is the reason for its greater resistance to the inhibitory peptides.

We matched Env densities in order to compare extents and kinetics of fusion induced by the WT and ΔCT. But it has been concluded that mutating the two cysteines of the CT so that Env can no longer become palmitoylated eliminates association of Env with rafts (3), and thus the WT and ΔCT may be distributed differently over the cell surfaces. The spatial distribution of Env, and other factors, could significantly affect the time course of the protein interactions necessary for fusion.

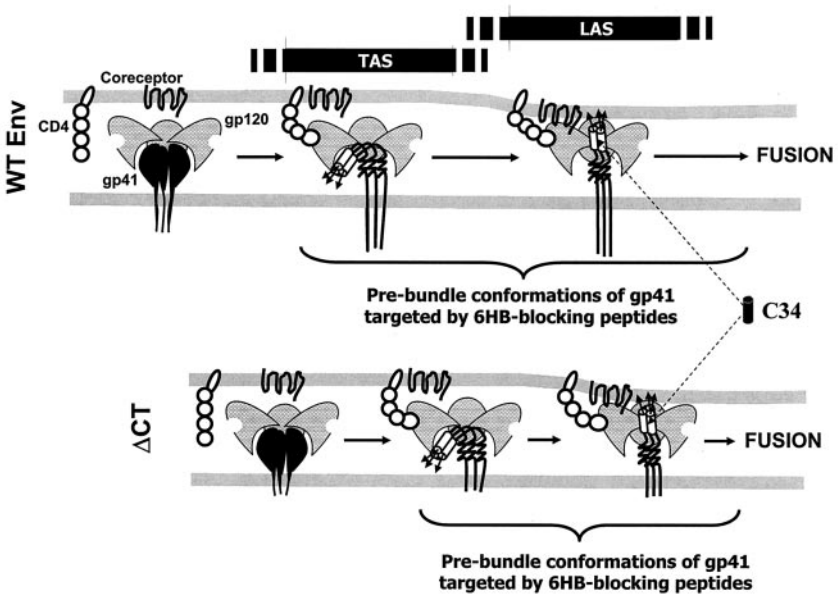

FIG. 8. The time from maximal groove exposure to formation of the 6HB is briefer for ΔCT. C34 inhibits WT-induced fusion more effectively than ΔCT-induced fusion at the TAS, indicating that the grooves of ΔCT are less well exposed than those of the WT at this stage. Inhibition of fusion by C34 is the same for the WT and ΔCT at the LAS. Once grooves are fully exposed, ΔCT more quickly folds into a 6HB, illustrated as shorter transition arrows between the TAS and the LAS and between the LAS and fusion for ΔCT. The progression from left to right denotes a reaction coordinate (rather than time) for fusion.

This limits the ability to use kinetics of fusion to draw conclusions concerning mechanisms of peptide inhibition of fusion. Our strategy of testing the potency of peptides at intermediate stages of fusion avoids this limitation.

The CT hinders conformational changes required for the prebundle to 6HB transition. Folding kinetics have been suggested as the primary determinant of the greater susceptibility of X4-tropic than R5-tropic Env to peptide inhibitors (48). The evidence was based on the finding that as V3 loop variants of Env exhibited faster fusion kinetics, resistance of fusion to T20 increased (48). Our results are consistent with that finding: C34 was a more effective inhibitor of X4-tropic HXB2 than of R5-tropic JRFL (Fig. 5A), and fusion kinetics were faster for JRFL than for HXB2 (Fig. 2). In addition to faster kinetics causing JRFL Env to reside in prebundle configurations for shorter times than HXB2, exposure of binding sites may occur later for JRFL: binding soluble CD4 exposes the coiled coil and C-terminal segments of HXB2 but not of JRFL Env (19). Another potential reason for reduced effectiveness of C34 against JRFL Env is that the amino acid sequence of C34 is the same as that of the HXB2 Env sequence, while the corresponding region of JRFL differs at five positions. However, a C34 derived from the sequence of SIV Env effectively inhibits HIV-1 Env (21, 41) and about half of the residues are different for HIV-1 and SIV C34 residues. It is therefore expected that C34 binds to HXB2 and JRFL with the same affinity. In addition, an alignment of helical wheels of HXB2 and JRFL residues shows that none of their differences occur at a or d positions and it is these positions that should fit into the grooves of the coiled coil.

Several lines of evidence suggest that the long CT stabilizes the native structure of the ectodomain of HIV Env (Fig. 4 and references 18, 45, and 58). On the basis of our data, the consequences of the presence of the CT are not limited to this initial structure but extend to conformational changes at the various steps of fusion. Importantly, the long CT slows, but does not prevent, the major conformational change necessary for the transition to the 6HB structure from a prebundle conformation in which grooves are maximally exposed. We envision that deletion of the CT increases the configurational freedom of Env during the fusion process. At some point in the fusion process, several trimers of Env probably come together to form a fusion complex. ΔCT may have a significantly higher mobility than the WT because the CT is large and/or because removing the palmitoyls of CT reduces interactions with the inner monolayer of the plasma membrane. A higher mobility of ΔCT could shorten the time required for cluster formation. The reduced time of groove exposure of ΔCT may thus be caused by faster folding of individual trimers into a 6HB bundle and/or by faster association among individual trimers. The finding that inhibition of fusion by C34 at the LAS is independent of Env density (Table 2) and the same for the WT and ΔCT suggests that Env trimers have already complexed among themselves into a fusion complex at the LAS and that the number of trimers within a complex is independent of surface density.

The kinetics of the WT and ΔCT from the TAS were the same for HXB2 Env (Fig. 2) but faster for ΔCT than for the WT in control experiments. This suggests that the kinetic advantages conferred by deleting the CT are used in early, rather than in late, steps of fusion. Because deleting the CT exposes chemokine binding sites of Env (18), it would be expected that ΔCT more quickly engages CXCR4 than does the WT. Faster engagement of CXCR4 may be the reason ΔCT speeds up the

early, pre-TAS steps. However, C34 was still more potent in inhibiting WT-induced fusion from the TAS, showing that rank ordering the rate of fusion for variants of Env does not reliably allow one to predict, or account for, the sequence of potency of inhibition of fusion by bundle-blocking peptides. In other words, differences in kinetics of fusion between variants can be caused by steps that are unrelated to bundle formation.

In comparing C34 and the 5-helix peptide, we found that as the fusion process progressed, inhibition by C34 remained the same or increased whereas inhibition by the 5-helix peptide decreased. Less accessibility of the C-terminal segments of Env to the 5-helix peptide as fusion proceeded could have resulted from the relatively large size of the peptide. Reduced inhibition of fusion at the LAS has also been observed for peptides directed against the groove-fitting C-terminal portion of SV5 F (52).

Interactions of the CT with viral and cellular components may influence membrane fusion. In the viral setting, the CT of HIV-1 Env interacts with Gag (45, 58). If the HIV-1 protease does not cleave Gag and Gag-Pol polyprotein precursors, the virus does not mature and remains noninfectious (24, 33, 47). But deleting the CT renders the virus infectious even if Gag and Gag-Pol remain uncleaved (45, 58). It has been concluded that the interaction between the CT and Gag of the immature virus prevents the virus from fusing to membranes; deleting the CT eliminates the interactions and allows fusion to proceed (45, 58). Our data suggest that deletion of the CT inherently improves the ability of the virus to fuse to and therefore to infect cells, independent of advantages conferred by dissociation of Env from Gag.

What molecular occurrence might account for the observation that eliminating the CT causes the grooves of the prebundle to be exposed for less time? In folding into a 6HB from a prebundle configuration, the three membrane-spanning domains of a gp41 trimer must separate from each other and move toward the fusion peptides inserted in the target membrane. We propose that the interactions between the long CT and viral or cellular components, or the large size of the CT, or a combination of these factors, reduce the freedom of movements of membrane-spanning domains. Deleting the CT eliminates these restrictions. Quicker folding of individual trimers from prebundles to bundles and/or any interactions between trimers would thus be facilitated by deletion of the CT.

ACKNOWLEDGMENTS

We thank Greg Spear for use of his flow cytometer and Sofya Brener for steady and excellent technical assistance. We thank Eric Hunter for critical reading of the manuscript and insightful comments. He also kindly provided the WT and ΔCT plasmids for HXB2.

This study was supported by National Institutes of Health grants GM27367, GM54787, and AI42382.

REFERENCES

1. **Abrahamyan, L. G., R. M. Markosyan, J. P. Moore, F. S. Cohen, and G. B. Melikyan.** 2003. Human immunodeficiency virus type 1 Env with an intersubunit disulfide bond engages coreceptors but requires bond reduction after engagement to induce fusion. J. Virol. **77:**5829–5836.
2. **Armand-Ugon, M., A. Gutierrez, B. Clotet, and J. A. Este.** 2003. HIV-1 resistance to the gp41-dependent fusion inhibitor C-34. Antiviral Res. **59:** 137–142.
3. **Bhattacharya, J., P. J. Peters, and P. R. Clapham.** 2004. Human immunodeficiency virus type 1 envelope glycoproteins that lack cytoplasmic domain cysteines: impact on association with membrane lipid rafts and incorporation onto budding virus particles. J. Virol. **78:**5500–5506.
4. **Binley, J. M., C. S. Cayanan, C. Wiley, N. Schulke, W. C. Olson, and D. R. Burton.** 2003. Redox-triggered infection by disulfide-shackled human immunodeficiency virus type 1 pseudovirions. J. Virol. **77:**5678–5684.
5. **Blacklow, S. C., M. Lu, and P. S. Kim.** 1995. A trimeric subdomain of the simian immunodeficiency virus envelope glycoprotein. Biochemistry **34:**14955–14962.
6. **Boge, M., S. Wyss, J. S. Bonifacino, and M. Thali.** 1998. A membrane-proximal tyrosine-based signal mediates internalization of the HIV-1 envelope glycoprotein via interaction with the AP-2 clathrin adaptor. J. Biol. Chem. **273:**15773–15778.
7. **Burton, D. R., C. F. Barbas III, M. A. Persson, S. Koenig, R. M. Chanock, and R. A. Lerner.** 1991. A large array of human monoclonal antibodies to type 1 human immunodeficiency virus from combinatorial libraries of asymptomatic seropositive individuals. Proc. Natl. Acad. Sci. USA **88:**10134–10137.
8. **Chakrabarti, L., M. Emerman, P. Tiollais, and P. Sonigo.** 1989. The cytoplasmic domain of simian immunodeficiency virus transmembrane protein modulates infectivity. J. Virol. **63:**4395–4403.
9. **Chan, D. C., D. Fass, J. M. Berger, and P. S. Kim.** 1997. Core structure of gp41 from the HIV envelope glycoprotein. Cell **89:**263–273.
10. **Chan, D. C., and P. S. Kim.** 1998. HIV entry and its inhibition. Cell **93:**681–684.
11. **Deng, H. K., D. Unutmaz, V. N. KewalRamani, and D. R. Littman.** 1997. Expression cloning of new receptors used by simian and human immunodeficiency viruses. Nature **388:**296–300.
12. **Derdeyn, C. A., J. M. Decker, J. N. Sfakianos, X. Wu, W. A. O'Brien, L. Ratner, J. C. Kappes, G. M. Shaw, and E. Hunter.** 2000. Sensitivity of human immunodeficiency virus type 1 to the fusion inhibitor T-20 is modulated by coreceptor specificity defined by the V3 loop of gp120. J. Virol. **74:**8358–8367.
13. **Derdeyn, C. A., J. M. Decker, J. N. Sfakianos, Z. Zhang, W. A. O'Brien, L. Ratner, G. M. Shaw, and E. Hunter.** 2001. Sensitivity of human immunodeficiency virus type 1 to fusion inhibitors targeted to the gp41 first heptad repeat involves distinct regions of gp41 and is consistently modulated by gp120 interactions with the coreceptor. J. Virol. **75:**8605–8614.
14. **Doms, R. W.** 2000. Beyond receptor expression: the influence of receptor conformation, density, and affinity in HIV-1 infection. Virology **276:**229–237.
15. **Eckert, D. M., and P. S. Kim.** 2001. Design of potent inhibitors of HIV-1 entry from the gp41 N-peptide region. Proc. Natl. Acad. Sci. USA **98:**11187–11192.
16. **Eckert, D. M., and P. S. Kim.** 2001. Mechanisms of viral membrane fusion and its inhibition. Annu. Rev. Biochem. **70:**777–810.
17. **Edwards, T. G., T. L. Hoffman, F. Baribaud, S. Wyss, C. C. LaBranche, J. Romano, J. Adkinson, M. Sharron, J. A. Hoxie, and R. W. Doms.** 2001. Relationships between CD4 independence, neutralization sensitivity, and exposure of a CD4-induced epitope in a human immunodeficiency virus type 1 envelope protein. J. Virol. **75:**5230–5239.
18. **Edwards, T. G., S. Wyss, J. D. Reeves, S. Zolla-Pazner, J. A. Hoxie, R. W. Doms, and F. Baribaud.** 2002. Truncation of the cytoplasmic domain induces exposure of conserved regions in the ectodomain of human immunodeficiency virus type 1 envelope protein. J. Virol. **76:**2683–2691.
19. **Furuta, R. A., C. T. Wild, Y. Weng, and C. D. Weiss.** 1998. Capture of an early fusion-active conformation of HIV-1 gp41. Nat. Struct. Biol. **5:**276–279.
20. **Gallo, S. A., A. Puri, and R. Blumenthal.** 2001. HIV-1 gp41 six-helix bundle formation occurs rapidly after the engagement of gp120 by CXCR4 in the HIV-1 Env-mediated fusion process. Biochemistry **40:**12231–12236.
21. **Gallo, S. A., K. Sackett, S. S. Rawat, Y. Shai, and R. Blumenthal.** 2004. The stability of the intact envelope glycoproteins is a major determinant of sensitivity of HIV/SIV to peptidic fusion inhibitors. J. Mol. Biol. **340:**9–14.
22. **Golding, H., M. Zaitseva, E. de Rosny, L. R. King, J. Manischewitz, I. Sidorov, M. K. Gorny, S. Zolla-Pazner, D. S. Dimitrov, and C. D. Weiss.** 2002. Dissection of human immunodeficiency virus type 1 entry with neutralizing antibodies to gp41 fusion intermediates. J. Virol. **76:**6780–6790.
23. **Gorny, M. K., A. J. Conley, S. Karwowska, A. Buchbinder, J. Y. Xu, E. A. Emini, S. Koenig, and S. Zolla-Pazner.** 1992. Neutralization of diverse human immunodeficiency virus type 1 variants by an anti-V3 human monoclonal antibody. J. Virol. **66:**7538–7542.
24. **Gottlinger, H. G., J. G. Sodroski, and W. A. Haseltine.** 1989. Role of capsid precursor processing and myristoylation in morphogenesis and infectivity of human immunodeficiency virus type 1. Proc. Natl. Acad. Sci. USA **86:**5781–5785.
25. **Hirsch, V. M., P. Edmondson, M. Murphey-Corb, B. Arbeille, P. R. Johnson, and J. I. Mullins.** 1989. SIV adaptation to human cells. Nature **341:**573–574.
26. **Hoffman, T. L., and R. W. Doms.** 1999. HIV-1 envelope determinants for cell tropism and chemokine receptor use. Mol. Membr. Biol. **16:**57–65.
27. **Hoffman, T. L., C. C. LaBranche, W. Zhang, G. Canziani, J. Robinson, I. Chaiken, J. A. Hoxie, and R. W. Doms.** 1999. Stable exposure of the coreceptor-binding site in a CD4-independent HIV-1 envelope protein. Proc. Natl. Acad. Sci. USA **96:**6359–6364.
28. **Huerta, L., E. Lamoyi, A. Baez-Saldana, and C. Larralde.** 2002. Human immunodeficiency virus envelope-dependent cell-cell fusion: a quantitative fluorescence cytometric assay. Cytometry **47:**100–106.
29. **Hung, C. S., N. Vander Heyden, and L. Ratner.** 1999. Analysis of the critical

domain in the V3 loop of human immunodeficiency virus type 1 gp120 involved in CCR5 utilization. J. Virol. **73:**8216–8226.
30. **Jaroszeski, M. J., R. Gilbert, and R. Heller.** 1994. Detection and quantitation of cell-cell electrofusion products by flow cytometry. Anal. Biochem. **216:** 271–275.
31. **Jonak, Z. L., R. K. Clark, D. Matour, S. Trulli, R. Craig, E. Henri, E. V. Lee, R. Greig, and C. Debouck.** 1993. A human lymphoid recombinant cell line with functional human immunodeficiency virus type 1 envelope. AIDS Res. Hum. Retroviruses **9:**23–32.
32. **Kilby, J. M., S. Hopkins, T. M. Venetta, B. DiMassimo, G. A. Cloud, J. Y. Lee, L. Alldredge, E. Hunter, D. Lambert, D. Bolognesi, T. Matthews, M. R. Johnson, M. A. Nowak, G. M. Shaw, and M. S. Saag.** 1998. Potent suppression of HIV-1 replication in humans by T-20, a peptide inhibitor of gp41-mediated virus entry. Nat. Med. **4:**1302–1307.
33. **Kohl, N. E., E. A. Emini, W. A. Schleif, L. J. Davis, J. C. Heimbach, R. A. Dixon, E. M. Scolnick, and I. S. Sigal.** 1988. Active human immunodeficiency virus protease is required for viral infectivity. Proc. Natl. Acad. Sci. USA **85:**4686–4690.
34. **Kwong, P. D.** 2004. The 447-52D antibody: hitting HIV-1 where its armor is thickest. Structure **12:**173–174.
35. **LaBranche, C. C., T. L. Hoffman, J. Romano, B. S. Haggarty, T. G. Edwards, T. J. Matthews, R. W. Doms, and J. A. Hoxie.** 1999. Determinants of CD4 independence for a human immunodeficiency virus type 1 variant map outside regions required for coreceptor specificity. J. Virol. **73:**10310–10319.
36. **Labrosse, B., J. L. Labernardiere, E. Dam, V. Trouplin, K. Skrabal, F. Clavel, and F. Mammano.** 2003. Baseline susceptibility of primary human immunodeficiency virus type 1 to entry inhibitors. J. Virol. **77:**1610–1613.
37. **Lin, G., B. Lee, B. S. Haggarty, R. W. Doms, and J. A. Hoxie.** 2001. CD4-independent use of rhesus CCR5 by human immunodeficiency virus type 2 implicates an electrostatic interaction between the CCR5 N terminus and the gp120 C4 domain. J. Virol. **75:**10766–10778.
38. **Lin, X., C. A. Derdeyn, R. Blumenthal, J. West, and E. Hunter.** 2003. Progressive truncations C terminal to the membrane-spanning domain of simian immunodeficiency virus Env reduce fusogenicity and increase concentration dependence of Env for fusion. J. Virol. **77:**7067–7077.
39. **Lineberger, J. E., R. Danzeisen, D. J. Hazuda, A. J. Simon, and M. D. Miller.** 2002. Altering expression levels of human immunodeficiency virus type 1 gp120-gp41 affects efficiency but not kinetics of cell-cell fusion. J. Virol. **76:**3522–3533.
40. **Maddon, P. J., A. G. Dalgleish, J. S. McDougal, P. R. Clapham, R. A. Weiss, and R. Axel.** 1986. The T4 gene encodes the AIDS virus receptor and is expressed in the immune system and the brain. Cell **47:**333–348.
41. **Malashkevich, V. N., D. C. Chan, C. T. Chutkowski, and P. S. Kim.** 1998. Crystal structure of the simian immunodeficiency virus (SIV) gp41 core: conserved helical interactions underlie the broad inhibitory activity of gp41 peptides. Proc. Natl. Acad. Sci. USA **95:**9134–9139.
42. **Markosyan, R. M., F. S. Cohen, and G. B. Melikyan.** 2003. HIV-1 envelope proteins complete their folding into six-helix bundles immediately after fusion pore formation. Mol. Biol. Cell **14:**926–938.
43. **Markosyan, R. M., X. Ma, M. Lu, F. S. Cohen, and G. B. Melikyan.** 2002. The mechanism of inhibition of HIV-1 Env-mediated cell-cell fusion by recombinant gp41 ectodomain cores. Virology **302:**174–184.
44. **Melikyan, G. B., R. M. Markosyan, H. Hemmati, M. K. Delmedico, D. M. Lambert, and F. S. Cohen.** 2000. Evidence that the transition of HIV-1 gp41 into a six-helix bundle, not the bundle configuration, induces membrane fusion. J. Cell Biol. **151:**413–424.
45. **Murakami, T., S. Ablan, E. O. Freed, and Y. Tanaka.** 2004. Regulation of human immunodeficiency virus type 1 Env-mediated membrane fusion by viral protease activity. J. Virol. **78:**1026–1031.
46. **Niwa, H., K. Yamamura, and J. Miyazaki.** 1991. Efficient selection for high-expression transfectants with a novel eukaryotic vector. Gene **108:**193–199.
47. **Peng, C., B. K. Ho, T. W. Chang, and N. T. Chang.** 1989. Role of human immunodeficiency virus type 1-specific protease in core protein maturation and viral infectivity. J. Virol. **63:**2550–2556.
48. **Reeves, J. D., S. A. Gallo, N. Ahmad, J. L. Miamidian, P. E. Harvey, M. Sharron, S. Pohlmann, J. N. Sfakianos, C. A. Derdeyn, R. Blumenthal, E. Hunter, and R. W. Doms.** 2002. Sensitivity of HIV-1 to entry inhibitors correlates with envelope/coreceptor affinity, receptor density, and fusion kinetics. Proc. Natl. Acad. Sci. USA **99:**16249–16254.
49. **Reeves, J. D., and T. F. Schulz.** 1997. The CD4-independent tropism of human immunodeficiency virus type 2 involves several regions of the envelope protein and correlates with a reduced activation threshold for envelope-mediated fusion. J. Virol. **71:**1453–1465.
50. **Root, M. J., and D. H. Hamer.** 2003. Targeting therapeutics to an exposed and conserved binding element of the HIV-1 fusion protein. Proc. Natl. Acad. Sci. USA **100:**5016–5021.
51. **Root, M. J., M. S. Kay, and P. S. Kim.** 2001. Protein design of an HIV-1 entry inhibitor. Science **291:**884–888.
52. **Russell, C. J., T. S. Jardetzky, and R. A. Lamb.** 2001. Membrane fusion machines of paramyxoviruses: capture of intermediates of fusion. EMBO J. **20:**4024–4034.
53. **Speck, R. F., K. Wehrly, E. J. Platt, R. E. Atchison, I. F. Charo, D. Kabat, B. Chesebro, and M. A. Goldsmith.** 1997. Selective employment of chemokine receptors as human immunodeficiency virus type 1 coreceptors determined by individual amino acids within the envelope V3 loop. J. Virol. **71:**7136–7139.
54. **Stanfield, R. L., M. K. Gorny, C. Williams, S. Zolla-Pazner, and I. A. Wilson.** 2004. Structural rationale for the broad neutralization of HIV-1 by human monoclonal antibody 447-52D. Structure **12:**193–204.
55. **Tan, K., J. Liu, J. Wang, S. Shen, and M. Lu.** 1997. Atomic structure of a thermostable subdomain of HIV-1 gp41. Proc. Natl. Acad. Sci. USA **94:** 12303–12308.
56. **Weissenhorn, W., A. Dessen, S. C. Harrison, J. J. Skehel, and D. C. Wiley.** 1997. Atomic structure of the ectodomain from HIV-1 gp41. Nature **387:** 426–430.
57. **Wunschmann, S., and J. T. Stapleton.** 2000. Fluorescence-based quantitative methods for detecting human immunodeficiency virus type 1-induced syncytia. J. Clin. Microbiol. **38:**3055–3060.
58. **Wyma, D. J., A. Kotov, and C. Aiken.** 2000. Evidence for a stable interaction of gp41 with $Pr55^{Gag}$ in immature human immunodeficiency virus type 1 particles. J. Virol. **74:**9381–9387.